

Effects of charge dopants in quantum spin Hall materials

Tomasz Dietl^{1,2,*}

¹*International Research Centre MagTop, Institute of Physics,
Polish Academy of Sciences, Aleja Lotnikow 32/46, PL-02668 Warsaw, Poland*

²*WPI Advanced Institute for Materials Research, Tohoku University, 2-1-1 Katahira, Aoba-ku, Sendai 980-8577, Japan*

Semiconductors' sensitivity to electrostatic gating and doping accounts for their widespread use in information communication and new energy technologies. It is demonstrated quantitatively and with no adjustable parameters that the presence of paramagnetic acceptor dopants elucidates a variety of hitherto puzzling properties of two-dimensional topological semiconductors at the topological phase transition and in the regime of the quantum spin Hall effect. The concepts of charge correlation, Coulomb gap, exchange interaction between conducting electrons and holes localized on acceptors, strong coupling limit of the Kondo effect, and bound magnetic polaron explain a short topological protection length, high hole mobilities compared with electron mobilities, and different temperature dependence of the spin Hall resistance in HgTe and (Hg,Mn)Te quantum wells.

Introduction—Quantized Hall resistance is a hallmark of two-dimensional (2D) topological electronic systems [1]. The integer quantum Hall effect's high-precision quantization is behind a new definition of units [2], whereas other quantum Hall phenomena lead to many far-reaching developments [1]. Surprisingly, however, although the quantum spin Hall effect (QSHE) has been known for more than a decade [3–5], experimental resistance magnitudes attain the expected value $h/2e^2$ only in mesoscopic samples, such as micron-size HgTe-based quantum wells (QWs) [6, 7] and sub-100-nm atomically thin 1T'-WTe₂ 2D monolayers [8, 9]. Moreover, although several theoretical models have been proposed [10], a short experimentally found protection length has usually been assigned [6–9] to unidentified "charge puddles" that trap edge carriers and within which spin-flip, allowing for scattering between helical edges, occurs [11].

We claim here that the challenging properties of QSHE semiconductors result from the presence of native acceptors in these materials. Accordingly, the starting point for this work is a quantitative theory of acceptor states in HgTe QWs, which provides positions of acceptor levels with respect to bands and topological edge states as a function of the QW thickness. With this information, we contend that the acceptor density is determined by the gate voltage range in which edge states carry the electric current [5–9, 12, 13]. Furthermore, considering charge correlation and Coulomb-gap effects [14], the acceptor scenario explains why at the 2D topological phase transition, the mobility of holes is significantly greater than that of electrons [15, 16], as well as elucidates the origin of high-frequency conductivity [17] and gating hystereses [13]. As a next step, a theory of exchange coupling between electrons and acceptor holes [18] is employed to demonstrate that, in topological materials, the interaction between edge electrons with acceptor holes reaches the strong coupling limit of the Kondo effect, where the spin dephasing rate assumes, up to a material-specific logarithmic correction, a universal behavior discussed in the context of magnetic impurities [19–21]. The central result of this work is that, in this limit, the topological protection length L_p in the Ohmic conductivity regime is given by a product of the inverse of one-dimensional (1D)

acceptor hole density in the edge region and the anisotropy of exchange coupling to hole spins. This finding elucidates the magnitude of L_p in HgTe QWs and WTe₂ 2D monolayers. Finally, we demonstrate that the formation of acceptor bound magnetic polarons explains a difference in carrier mobilities and the temperature dependence of the edge resistivity of topological HgTe and Hg_{1-x}Mn_xTe QWs [7]. The result presented here are supported and extended in the companion paper [22].

Acceptor levels—Native acceptors in compound semiconductors are frequently assigned to metal vacancies giving resulting in double acceptors ($Z = -2$) in II-VI materials, even though the case of ZnTe and CdTe show that residual substitutional impurities, such as Cu ($Z = -1$), are involved [23]. To describe acceptor states, a four-band $\vec{k} \cdot \vec{p}$ theory developed for acceptors in GaAs and HgTe QWs [24, 25] is extended in this report to the case, where eight bands are relevant [26], as discussed in detail in the companion paper [22]. Within the axial approximation, the component of the total angular momentum perpendicular the QW plane commutes with the Hamiltonian, meaning that the corresponding integer quantum number m can be used to label acceptor states. For the relevant D_{2d} symmetry and $Z = -1$, the ground-state Kramers doublet corresponds to either $m = 0$ and $m = -1$ or $m = 1$ and $m = -2$. The corresponding binding energies are denoted $E_{1/2}$ or $E_{3/2}$ as the corresponding wave functions are mainly composed of $p_{\pm 1/2}$ and $s_{\pm 1/2}$ or $p_{\pm 3/2}$ Kohn-Luttinger amplitudes, respectively.

Figure 1 depicts energies of relevant QW bands and acceptor ground-state levels for a range of the HgTe QW widths d_{QW} with colors representing a fraction of the $p_{\pm 3/2}$ amplitude in the carrier wave function. Three distinct areas are observed in Fig. 1(c): (i) normal band ordering (cation s states above anion p states) at small d_{QW} values; (ii) the range of the topological phase transition centered around the bandgap $E_g = 0$ and $d_c \approx 5.8$ nm; (iii) the topological region $d_w > d_c$, where the band ordering is inverted, resulting in 1D topological gapless edge states [3, 5] to be discussed later. Such a band diagram is generic for this class of 2D topological systems, however the value of d_c depends on strain (set to zero

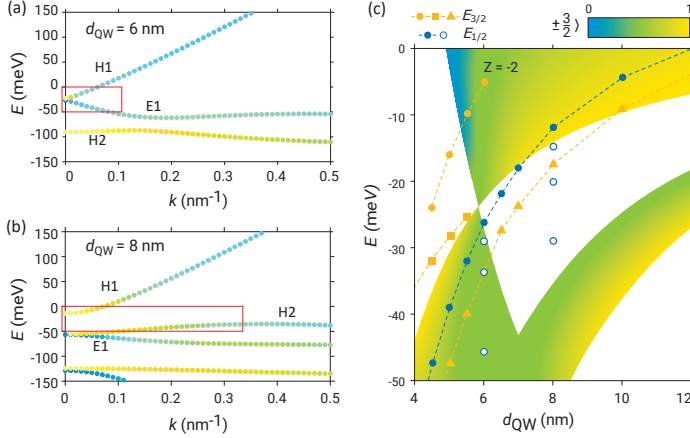


FIG. 1. Band structure and positions of acceptor levels in HgTe QWs of different thicknesses. (a, b) Band energies E vs. wavevector k for unstrained QW thickness of 6 and 8 nm sandwiched between $\text{Hg}_{0.3}\text{Cd}_{0.7}\text{Te}$ barriers. Red rectangles depict the band region displayed in (c). (c) Band edges and acceptor levels (symbols connected by dashed lines vs. QW thickness d_{QW}). Except for the orange circles computed for the doubly ionized acceptor ($Z = -2$), other symbols represent the single acceptor ($Z = -1$). The orange symbols ($E_{3/2}$) correspond to acceptors associated with the valence band around $k = 0$; the blue symbols ($E_{1/2}$) with valence band side maxima visible in (a) and (b). Full symbols represent the acceptors residing in the QW center; the open symbols represent acceptors at the distances $d_{QW}/4$, $d_{QW}/2$, and $3d_{QW}/2$ of the QW center. Colors represent the participation of the $p_{\pm 3/2}$ Kohn-Luttinger amplitude in the wave functions.

here) and Cd or Mn content in the barriers and well [15, 22].

We note that the binding energies of the doubly ionized acceptors $E^{(2-/-)}$ are irrelevant for the low-energy physics. In contrast, $E^{(-/0)}$ levels, residing near band edges or in the gap, are essential. They originate from either single acceptors ($Z = -1$) or singly ionized double acceptors that, in the mean-field approach, have the same binding energy as single acceptors. As seen in Fig. 1(c), in the regions of interest here ($d_{QW} \approx d_c$ and $d_{QW} > d_c$), the ground state corresponds to the level $E_{1/2}$ associated with the side maximum of the valence band visible in Figs. 1(a) and 1(b). Notably, the acceptor levels form a band, as the hole binding energy depends on the location of the parent acceptor impurity with respect to the QW center, as shown in Fig. 1(c).

Within this model, the range of gate voltage E_g at $d_{QW} > d_c$ directly provides the 2D areal density of relevant acceptors N_a , with the experimental data implying $N_a \approx 10^{11} \text{ cm}^{-2}$ for HgTe QWs [6, 16] and $N_a \approx 10^{13} \text{ cm}^{-2}$ for WTe_2 [8]. The value for the acceptor band in HgTe QWs corresponds to the three dimensional (3D) concentration of the order of $N_A = 3 \cdot 10^{16} \text{ cm}^{-3}$, a typical magnitude for bulk HgTe [27] and $\text{Hg}_{1-x}\text{Mn}_x\text{Te}$ [28]. For such a concentration the holes are localized, as for the evaluated Bohr radius of 5 nm, the Mott critical concen-

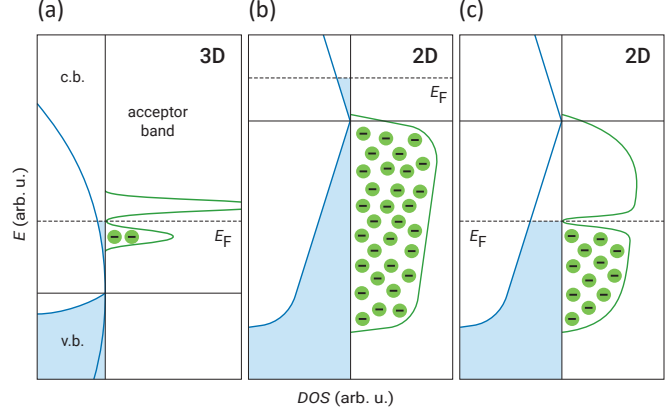


FIG. 2. Schematic picture of carrier and acceptor bands at the topological phase transition ($E_g = 0$). (a) Bulk 3D case with the Fermi energy pinned in the conduction band (c.b.) by acceptors negatively charged below the Fermi level. Coulomb gap at E_F is also shown. (b,c) The same for the 2D case and two positions of the Fermi level. The acceptor band is wide as the binding energy depends on the acceptor location with respect to the QW center.

tration is $1.4 \cdot 10^{17} \text{ cm}^{-3}$. Next, we demonstrate that the presence of acceptors explains several hitherto puzzling properties of 2D topological insulators.

Region of topological phase transition—One of the rather surprising facts is that low-temperature electron mobility μ_e in modulation donor-doped HgTe QWs d_{QW} barely reaches $0.4 \cdot 10^6 \text{ cm}^2/\text{Vs}$ [6], whereas μ_e in bulk HgTe as well as in $\text{Hg}_{1-x}\text{Cd}_x\text{Te}$ and $\text{Hg}_{1-x}\text{Mn}_x\text{Te}$ near the 3D topological transition approaches or exceeds $1 \cdot 10^6 \text{ cm}^2/\text{Vs}$ [27–29] with the onset of the Shubnikov de Haas oscillations at 10 mT [28]. Even more surprisingly, in the vicinity of the topological phase transition in 2D QWs, the hole mobility μ_h is larger than μ_e [15, 16], reaching $\mu_h = 0.9 \cdot 10^6 \text{ cm}^2/\text{Vs}$, for which the QHE plateau is resolved in 50 mT in $\text{Hg}_{0.976}\text{Mn}_{0.024}\text{Te}$ [15], which is relevant for the QHE metrology [16]. In addition, the QW hole concentration evaluated from the Hall effect, is significantly smaller than the charge density generated by the gate voltage [15, 16].

Figure 2 elucidates those findings using information obtained from Fig. 1. In the 3D bulk case (Fig. 2(a)), as previously discussed in detail [14], the acceptor band resides in the conduction band. In addition, due to a small electron mass value, we are on the metallic side of the Anderson-Mott transition so that donors do not bind electrons at any position of the Fermi energy E_F . Now, if the donor concentration $N_D \ll N_A$, most of the acceptors are neutral. Furthermore, under these conditions, to reduce the Coulomb energy, only acceptors in close vicinity to donors are ionized. The resulting dipole formation substantially reduces the electron scattering rate. Furthermore, the presence of the Efros-Shklovskii Coulomb gap precludes resonant scattering. By

fine hydrostatic pressure tuning of the band structure toward the 3D topological transition at $E_g = 0$, $\mu_e = 20 \cdot 10^6 \text{ cm}^2/\text{Vs}$ was registered in $\text{Hg}_{0.94}\text{Mn}_{0.06}\text{Te}$ at 2 K [28].

The situation is entirely different at the topological phase transition in the 2D case. As shown in Fig. 2(b), for the Fermi level in the conduction band, obtained through modulation donor doping, all acceptors are ionized, explaining the low electron mobility. In contrast, in the hole transport regime (Fig. 2(c)), achieved by gating-induced discharging of acceptors, the aforementioned charge correlation occurs, which along with the small effective mass of holes in the Dirac cone and the formation of the Coulomb gap E_C , results in high hole mobilities at $k_B T < E_C \approx 0.3 \text{ meV}$ [22]. Higher carrier mobility in Mn-containing samples [15, 28] compared to the HgTe case may not be accidental: E_C is enlarged by the acceptor bound magnetic polaron (BMP) energy E_p , where for $x_{\text{Mn}} = 0.02$, $E_p > 0.3 \text{ meV}$ at $T < 2 \text{ K}$ [22]. The Coulomb gap model explains also a large thermal stability of the QSHE in WTe_2 [9, 22].

Edge transport range—Having elucidated the role of acceptors in the region of the topological phase transition we focus on the region $d_{\text{QW}} > d_c$ (Fig. 2(c)). Here, the Coulomb gap diminishes d. c. hopping conductivity. However, since there is no Coulomb gap for electron–hole excitations, the presence of the acceptor band explains the origin of puzzling gap states detected by high-frequency conductivity [17]. Moreover, under these conditions, one can anticipate the appearance of the exchange interaction \mathcal{H}_{eh} between spins of electrons in the topological edge states, \vec{s} , and paramagnetic acceptor holes, \vec{J} .

To reveal the striking consequences of this suggestion, it worth recalling that a long-range component of this coupling originates from the third order perturbation theory (second in kp and first in the Coulomb interaction), for which the exchange energy $\mathcal{J}_{eh} \propto 1/E_{eh}^2$, where E_{eh} represents the electron–hole energy distance. According to the theory [18], which is quantitatively verified for the interaction between photoelectrons at the bottom of the conduction and holes on Mn acceptors in GaAs [30], \mathcal{H}_{eh} assumes a scalar (Heisenberg) form, $\mathcal{H}_{eh} = -\mathcal{J}_{eh} \vec{s} \cdot \vec{J}$, where $J = 3/2$ and $\mathcal{J}_{eh} = -0.23 \text{ eV}$ [18]. When $E_{eh} = 1.4 \text{ eV}$ in GaAs:Mn, the lower bound of E_{eh} is as small as $E_C \approx 0.3 \text{ meV}$ for the topological edge electrons and acceptor holes. Hence, the antiferromagnetic \mathcal{J}_{eh} is the largest relevant energy, and despite a small DOS magnitude at E_F in the 1D channels, drives the system to a strong coupling limit of the Kondo effect [22], specified in QWs by a wide distribution of Kondo temperatures T_K . For the parameter values specifying HgTe QWs, i.e., the Fermi velocity $v_F = 4 \cdot 10^5 \text{ m/s}$ and the penetration length of the edge electron wave function into the QW, $b = 5 \text{ nm}$, a broad distribution of T_K values up to 100 K is expected [22]. Importantly, for areal hole density $N_a = 0.5 \cdot 10^{11} \text{ cm}^{-2}$, the number of edge electrons per unit length for E_F in the gap center $N_e = E_g/2\pi\hbar v_F = 12/\mu\text{m}$ is greater than the number of acceptor holes in the edge region, $N_h = N_a b = 3/\mu\text{m}$. This would also be the case of the double acceptors for which,

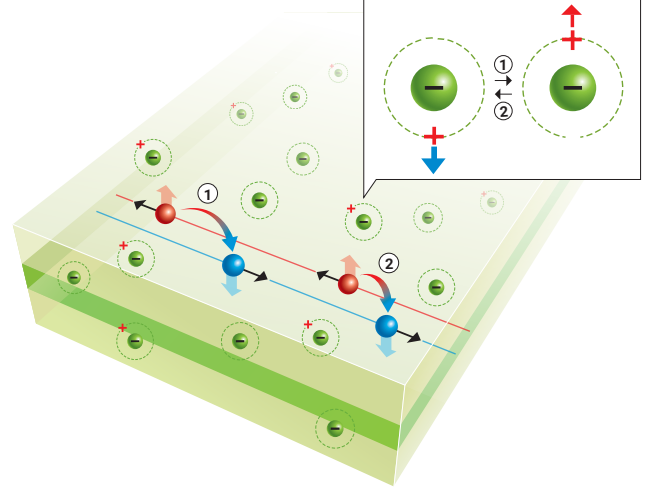


FIG. 3. Destructive role of charge dopants in the quantum spin Hall effect. If axial symmetry is maintained ($\mathcal{J}_x = \mathcal{J}_y$, $\mathcal{J}_{yz} = 0$, $D_x = 0$) only spin-flop ($\uparrow\downarrow \rightleftharpoons \downarrow\uparrow$) transitions occur (case 1 in the figure), so that edge current is conserved in the spin–momentum locking situation. However, if exchange interaction is anisotropic, $\uparrow\uparrow \rightleftharpoons \downarrow\downarrow$ spin nonconserving transitions are also allowed (case 2), leading to net backscattering after a chain of spin-dependent interactions of electrons with an acceptor.

if the Hund’s rule is obeyed, $N_h = 2N_a b$, independently of E_F .

Thus, we can quantitatively verify numerous theoretical studies on the Kondo effect in QSHE materials [19, 20, 31, 32]. It worth noting in this context that for transition metal impurities such as Mn, $T_K \ll 1 \text{ mK}$ in HgTe QWs [22].

More specifically [22], since the edge breaks the axial symmetry and a random distribution of holes the inversion symmetry, the exchange hamiltonian between edge electrons and acceptor holes $j = 1/2$ is not longer scalar but contains anisotropic terms, $\mathcal{J}_x - \mathcal{J}_y$, \mathcal{J}_{yz} , and D_x , the x -component of the Moriya-Dzyaloshinskii vector. For helical states with spin–momentum locking, exchange anisotropy ensures the leak of electron spin momentum to crystal orbital momentum in a chain of scattering events, resulting in net carrier backscattering [20, 31, 33], as sketched in Fig. 3. The resulting backscattering rate, compared to the conventional spin dephasing rate γ_s , is reduced by a factor r , so that $\gamma_b = r\gamma_s$, where $r = [2\mathcal{J}_{an}/((\mathcal{J}_x + \mathcal{J}_y))^2]$ [20, 33]. Importantly, evaluation of the Kondo temperature T_K for the system of acceptor hole spins and edge electrons indicates that the strong coupling regime can be reached in experimentally relevant temperature range [22]. In contrast, no Kondo effect is expected for impurities such as Mn [22, 33]. Thus, inverse L_p can be written in a simple form,

$$L_p^{-1} = \sum_i r^{(i)} f(T/T_K^{(i)})/L_x, \quad (1)$$

where the summation is over all QW holes bound to acceptors for a given gate voltage V_g . The function $F(x) = 1$ for $x = 1$, it decays to zero for $x \rightarrow 0$ and slowly decreases with x for $x > 1$ (for $x = 0.2$ and 10 , $F(x) = 0.5$ and 0.6 , respectively) [21]. The r value is not universal, but varies with the hole position in respect to the edge and QW center. To estimate L_p we adopt [22]: the areal hole density as $N_a = 0.5 \cdot 10^{11} \text{ cm}^{-2}$, an average value of $r^{(i)}$ as $r_{Dx} = 0.13$, the cut-off length beyond which strong coupling of holes and electrons tends to vanish $y_c = 2b = 10 \text{ nm}$, and an average value of $f(T/T_K) = 0.4$. These numbers lead to $L_p = 4 \mu\text{m}$, the order of magnitude consistent with experimental findings [5, 13, 34]. A more elaborated approach [22] provides conductance values and temperature dependence $G(T)$ that agree with experimental observations if the influence of Luttinger correlation effects upon r is taken into account [35].

An unexpected appearance of quantized resistance below 0.3 K in a $\text{Hg}_{0.988}\text{Mn}_{0.012}\text{Te}$ QW [7] can be elucidated using the acceptor model by spin splitting Δ of hole states originating from the BMP effect, as for $x = 0.012$, $\Delta > k_B T$ at $T < 3.5 \text{ K}$ [22]. Interestingly, the existing theories on the disappearance of the Kondo effect in a magnetic field assume the same Δ for the impurity and band states [36], which is not the case in the presence of BMPs.

Furthermore, a small number of relevant acceptor holes leads to reproducible resistance fluctuations [5, 7–9]. At the same time, elementary charging and discharging of barrier acceptors under a strong gate electric field may account for hysteretic and irreversibilities in low-temperature transport properties when cycling the gate voltage [7, 13].

Conclusions—The proposed acceptor impurity band model can elucidate the critical properties of QSHE materials. The presented results point to a dual role of charge dopants. On the one hand, they enlarge the plateau width, and on the other diminish the quantization precision. However, the resistance quantization accuracy can be recovered by doping topological QWs with magnetic impurities, as the formation of the bound magnetic polarons weakens the Kondo effect. In this paper, the model's quantitative predictions have been compared to experimental data on HgTe and $\text{Hg}_{1-x}\text{Mn}_x\text{Te}$ QWs as well as on $1\text{T}'\text{-WTe}_2$ 2D monolayers, however, it would be interesting to verify the model in the case of other QSHE candidate materials, such as $\alpha\text{-Sn}$ and Bi films, other 2D monolayers, and Heusler compounds with an inverted band structure. More generally, while electrostatic gating is widely used to reveal the unique properties of quantum materials, the results presented here demonstrate that charge dopants play an important and unanticipated role in the physics and applications of topological semiconductors. Finally, we mention that our theory have been limited to the Ohmic range. A number of new phenomena are expected beyond the linear response regime [35, 37, 38].

Acknowledgments—This project was supported by the Foundation for Polish Science through the International Research Agendas program co-financed by the European Union within the Smart Growth Operational Programme.

* dietl@MagTop.ifpan.edu.pl

- [1] K. von Klitzing, T. Chakraborty, P. Kim, V. Madhavan, Xi Dai, J. McIver, Y. Tokura, L. Savary, D. Smirnova, A. M. Rey, C. Felser, J. Gooth, and Xiaoliang Qi, “40 years of the quantum Hall effect,” *Nat. Rev. Phys.* **2**, 397–401 (2020).
- [2] A. F. Rigosi and R. E. Elmquist, “The quantum Hall effect in the era of the new SI,” *Semicon. Sci. Techn.* **34**, 093004 (2019).
- [3] C. L. Kane and E. J. Mele, “Quantum spin Hall effect in graphene,” *Phys. Rev. Lett.* **95**, 226801 (2005).
- [4] B. A. Bernevig, T. L. Hughes, and Shou-Cheng Zhang, “Quantum spin Hall effect and topological phase transition in HgTe quantum wells,” *Science* **314**, 1757–1761 (2006).
- [5] M. König, S. Wiedmann, C. Brüne, A. Roth, H. Buhmann, L. W. Molenkamp, Xiao-Liang Qi, and Shou-Cheng Zhang, “Quantum spin Hall insulator state in HgTe quantum wells,” *Science* **318**, 766–770 (2007).
- [6] K. Bendias, S. Shamim, O. Herrmann, A. Budewitz, P. Shekhar, P. Leubner, J. Kleinlein, E. Bocquillon, H. Buhmann, and L. W. Molenkamp, “High mobility HgTe microstructures for quantum spin Hall studies,” *Nano Lett.* **18**, 4831–4836 (2018).
- [7] S. Shamim, W. Beugeling, P. Shekhar, K. Bendias, L. Lunczer, J. Kleinlein, H. Buhmann, and L. W. Molenkamp, “Quantized spin Hall conductance in a magnetically doped two dimensional topological insulator,” *Nat. Commun.* **12**, 3193 (2021).
- [8] Zaiyao Fei, T. Palomaki, Sanfeng Wu, Wenjin Zhao, Xinghan Cai, Bosong Sun, Paul Nguyen, J. Finney, Xiaodong Xu, and D. H. Cobden, “Edge conduction in monolayer WTe_2 ,” *Nat. Phys.* **13**, 677–682 (2017).
- [9] Sanfeng Wu, V. Fatemi, Q. D. Gibson, K. Watanabe, T. Taniguchi, R. J. Cava, and P. Jarillo-Herrero, “Observation of the quantum spin Hall effect up to 100 kelvin in a monolayer crystal,” *Science* **359**, 76–79 (2018).
- [10] O. M. Yevtushenko and V. I. Yudson, “Protection of edge transport in quantum spin Hall samples: spin-symmetry based general approach and examples,” *New J. Phys.* **24**, 023040 (2022).
- [11] J. I. Väyrynen, M. Goldstein, Y. Gefen, and L. I. Glazman, “Resistance of helical edges formed in a semiconductor heterostructure,” *Phys. Rev. B* **90**, 115309 (2014).
- [12] G. Grabecki, J. Wróbel, M. Czapkiewicz, Ł. Cywiński, S. Gierałtowska, E. Guziewicz, M. Zholudev, V. Gavrilenko, N. N. Mikhailov, S. A. Dvoretzki, F. Teppe, W. Knap, and T. Dietl, “Nonlocal resistance and its fluctuations in microstructures of band-inverted $\text{HgTe}/(\text{Hg,Cd})\text{Te}$ quantum wells,” *Phys. Rev. B* **88**, 165309 (2013).
- [13] L. Lunczer, P. Leubner, M. Endres, V. L. Müller, C. Brüne, H. Buhmann, and L. W. Molenkamp, “Approaching quantization in macroscopic quantum spin Hall devices through gate training,” *Phys. Rev. Lett.* **123**, 047701 (2019).
- [14] Z. Wilamowski, K. Świątek, T. Dietl, and J. Kossut, “Resonant states in semiconductors: A quantitative study of HgSe:Fe ,” *Solid State Commun.* **74**, 833–837 (1990).
- [15] S. Shamim, W. Beugeling, J. Böttcher, P. Shekhar, A. Budewitz, P. Leubner, L. Lunczer, E. M. Hankiewicz, H. Buhmann, and L. W. Molenkamp, “Emergent quantum Hall effects below 50 mT in a two-dimensional topological insulator,” *Adv. Sci.* **6**, eaba4625 (2020).
- [16] I. Yahniuk, A. Kazakov, B. Jouault, S. S. Krishtopenko, S. Kret, G. Grabecki, G. Cywiński, N. N. Mikhailov, S. A. Dvoretzki, J. Przybytek, V. I. Gavrilenko, F. Teppe, T. Dietl, and W. Knap, “ HgTe quantum wells for QHE metrology under soft cryomagnetic conditions: permanent magnets and liquid ^4He tempera-

- tures,” 10.48550/arXiv.2111.07581.
- [17] M. C. Dartiailh, S. Hartinger, A. Gourmelon, K. Bendias, H. Bartolomei, H. Kamata, J.-M. Berroir, G. Fève, B. Plaçais, L. Lunczer, R. Schlereth, H. Buhmann, L. W. Molenkamp, and E. Bocquillon, “Dynamical separation of bulk and edge transport in HgTe-based 2D topological insulators,” *Phys. Rev. Lett.* **124**, 076802 (2020).
- [18] C. Śliwa and T. Dietl, “Electron-hole contribution to the apparent $s - d$ exchange interaction in III-V dilute magnetic semiconductors,” *Phys. Rev. B* **78**, 165205 (2008).
- [19] J. Maciejko, Chaoxing Liu, Y. Oreg, Xiao-Liang Qi, Congjun Wu, and Shou-Cheng Zhang, “Kondo effect in the helical edge liquid of the quantum spin Hall state,” *Phys. Rev. Lett.* **102**, 256803 (2009).
- [20] Y. Tanaka, A. Furusaki, and K. A. Matveev, “Conductance of a helical edge liquid coupled to a magnetic impurity,” *Phys. Rev. Lett.* **106**, 236402 (2011).
- [21] T. Micklitz, A. Altland, T. A. Costi, and A. Rosch, “Universal dephasing rate due to diluted Kondo impurities,” *Phys. Rev. Lett.* **96**, 226601 (2006).
- [22] T. Dietl, “Quantitative theory of backscattering in topological HgTe and (Hg,Mn)Te quantum wells: acceptor states, Kondo effect, precessional dephasing, and bound magnetic polaron,” 10.48550/ arXiv.2209.03283.
- [23] J.L. Pautrat, J.M. Francou, N. Magnea, E. Molva, and K. Saminadayar, “Donors and acceptors in tellurium compounds; the problem of doping and self-compensation,” *J. Cryst. Growth* **72**, 194–204 (1985).
- [24] S. Fraizzoli and A. Pasquarello, “Infrared transitions between shallow acceptor states in GaAs-Ga_{1-x}Al_xAs quantum wells,” *Phys. Rev. B* **44**, 1118–1127 (1991).
- [25] D. V. Kozlov, V. V. Rumyantsev, and S. V. Morozov, “Spectra of double acceptors in layers of barriers and quantum wells of HgTe/CdHgTe heterostructures,” *Semiconductors* **53**, 1198–1202 (2019).
- [26] E. G. Novik, A. Pfeuffer-Jeschke, T. Jungwirth, V. Latussek, C. R. Becker, G. Landwehr, H. Buhmann, and L. W. Molenkamp, “Band structure of semimagnetic Hg_{1-y}Mn_yTe quantum wells,” *Phys. Rev. B* **72**, 035321 (2005).
- [27] K. Szlenk, “Temperature dependence of electron concentration in intrinsic-like HgTe,” *phys. stat. sol. (b)* **95**, 445–452 (1979).
- [28] M. Sawicki, T. Dietl, W. Plesiewicz, P. Sękowski, L. Śniadower, M. Baj, and L. Dmowski, in *Application of High Magnetic Fields in Physics of Semiconductors*, edited by G. Landwehr (Springer, Berlin, 1983) pp. 382-385.
- [29] J.J. Dubowski, T. Dietl, W. Szymańska, and R.R. Gałzka, “Electron scattering in Cd_xHg_{1-x}Te,” *J. Phys. Chem. Solids* **42**, 351–362 (1981).
- [30] R. C. Myers, M. Poggio, N. P. Stern, A. C. Gossard, and D. D. Awschalom, “Antiferromagnetic $s-d$ exchange coupling in GaMnAs,” *Phys. Rev. Lett.* **95**, 017204 (2005).
- [31] B. L. Altshuler, I. L. Aleiner, and V. I. Yudson, “Localization at the edge of a 2D topological insulator by Kondo impurities with random anisotropies,” *Phys. Rev. Lett.* **111**, 086401 (2013).
- [32] E. Eriksson, “Spin-orbit interactions in a helical luttinger liquid with a Kondo impurity,” *Phys. Rev. B* **87**, 235414 (2013).
- [33] L. Kimme, B. Rosenow, and A. Brataas, “Backscattering in helical edge states from a magnetic impurity and Rashba disorder,” *Phys. Rev. B* **93**, R081301 (2016).
- [34] M. M. Majewicz, *Nanostructure fabrication and electron transport studies in two-dimensional topological insulators (in Polish)*, Ph.D. thesis, Insitute of Physics, Polish Academy of Sciences (2019), unpublished.
- [35] J. I. Väyrynen, F. Geissler, and L. I. Glazman, “Magnetic moments in a helical edge can make weak correlations seem strong,” *Phys. Rev. B* **93**, 241301 (2016).
- [36] M. Filippone, C. P. Moca, A. Weichselbaum, J. von Delft, and C. Mora, “At which magnetic field, exactly, does the Kondo resonance begin to split? a Fermi liquid description of the low-energy properties of the Anderson model,” *Phys. Rev. B* **98**, 075404 (2018).
- [37] A. M. Lunde and G. Platero, “Helical edge states coupled to a spin bath: Current-induced magnetization,” *Phys. Rev. B* **86**, 035112 (2012).
- [38] A. Del Maestro, T. Hyart, and B. Rosenow, “Backscattering between helical edge states via dynamic nuclear polarization,” *Phys. Rev. B* **87**, 165440 (2013).